AD-A072 067 FLORIDA ATLANTIC UNIV BOCA RATON DEPT OF OCEAN ENGIN--ETC F/G 11/6
FATIGUE AND CORROSION FATIGUE OF HY-80 STEEL, AS APPLICABLE TO --ETC(U)
JUL 79 W H HARTT, J H ADAMSON N00014-78-C-0307

UNCLASSIFIED NL

| OF |

AD
A072067

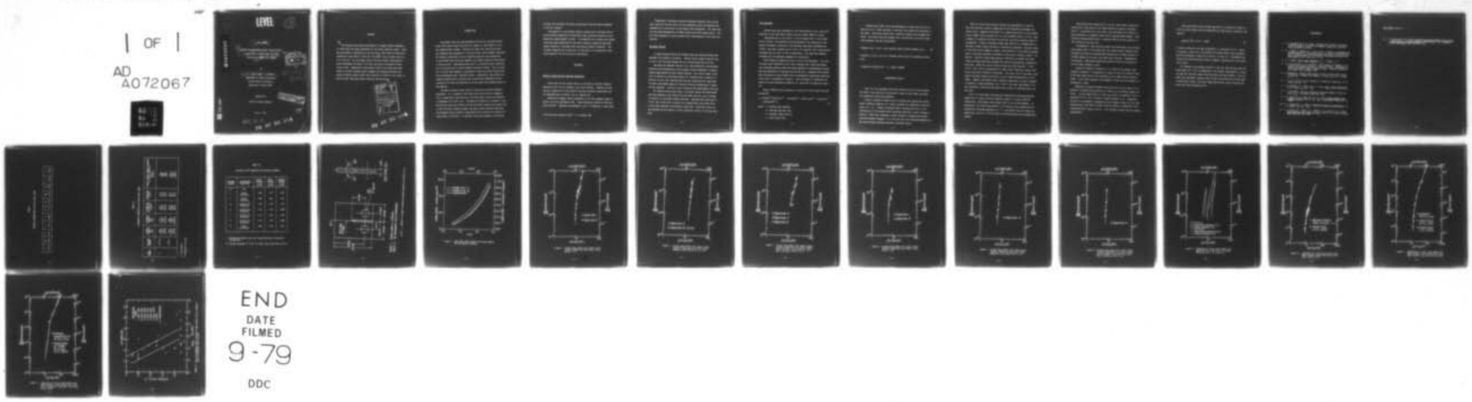

END
DATE
FILMED
9-79
DDC

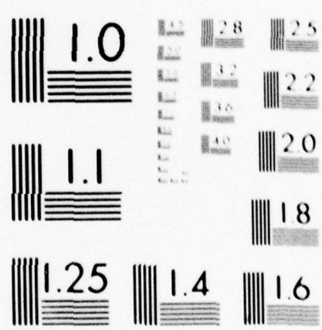

MICROCOPY RESOLUTION TEST CHART

9 FINAL REPORT

6

FATIGUE AND CORROSION FATIGUE OF HY-80 STEEL, AS APPLICABLE TO ANCHOR BOLT FAILURES

(Contract No. 15 N00014-78-C-0307 New

by

10 W. H. Hartt ~~and~~ J. H. Adamson
Department of Ocean Engineering
Florida Atlantic University
Boca Raton, Florida 33431

11 7 Jul 79

12 28p.

submitted to

Office of Naval Research

July 7, 1979

JOB

ABSTRACT

The fatigue crack growth rate behavior of compact tension specimens of HY-80 steel have been determined for low stress intensity ranges. Tests were performed in laboratory air and sea water, both freely corroding and cathodically polarized to -0.85 volts (Cu-$CuSO_4$), and at stress ratios, R, of 0.1 and 0.8. For the lowest stress intensity ranges investigated apparent thresholds for tests in air were less than in sea water at both stress ratios. Comparison of the present results with those upon other steels of various strength levels suggests that improved fatigue crack growth resistance should result from selection of HY-80 for low stress intensity range, high mean stress intensity applications.

INTRODUCTION

The present study has been prompted by failure of structural steel anchor bolts which secure guy wires for support of radio towers of military communication systems. Analysis of anchor bolt fracture surfaces has suggested that propagation of fatigue cracks, which probably developed from defects associated with the threading operation, was responsible. In the present application the eyebolts are loaded statically from tension in the guy wires. Superimposed upon this is a relatively small amplitude cyclic stressing due to cable strumming from wind loading. Thus, the eyebolt failures were probably a consequence of many low stress fatigue loadings superimposed upon a high mean stress. Additionally, the process was probably complicated by corrosion due to the marine atmosphere and the opportunity for salts and moisture to collect about the threaded region of the eyebolts.

The above situation lends itself to analysis by fracture mechanics techniques. It is assumed on this basis that the entirety of component life is comprised of the time for an initially small crack-like defection to propagate to critical size. The material properties of interest in predicting this particular failure include corrosion fatigue crack growth rate in the low stress intensity range, high mean stress intensity regime and the threshold stress intensity range below which fatigue and corrosion fatigue cracks do not grow. In addition, since such hardware is often gal-

vanized, the influence of cathodic polarization upon the above parameters is also of interest.

The objective of the present research project was to evaluate the corrosion fatigue properties of HY-80 steel under conditions relevant to communication system eyebolt failures. To accomplish this fatigue crack growth rates have been determined for low stress intensity ranges and high mean stress intensity in sea water with and without cathodic protection. The ultimate intension was to disclose if HY-80 steel is an appropriate alternative material for this particular application.

PROCEDURE

Material Properties and Specimen Preparation

HY-80 stock for the present tests was provided by the Naval Research Laboratory from 10.2 cm. diameter, half-round forgings. Chemistry and mechanical properties for this material had been previously determined* and are presented here as Tables I and II, respectively.

Machining of compact tension specimens to the final geometry shown in Figure 1 was also performed by NRL. These dimensions conform to ASTM Standard E 647-78T. Specimens corresponded to the L-T orientation in each case.

* This data was obtained from Mr. T. W. Crooker, NRL.

Preparation of specimens involved scratching reference lines 2.54 mm apart starting from the notch root and proceeding across the specimen face perpendicular to the plane of anticipated crack propagation. This same face was then metallographically polished through one micron diamond paste. This was found necessary to insure optimum visual determination of the crack tip location.

Sea Water Testing

A closed plexiglas-Devcon 30 (Flexane) bath was fabricated about each specimen to be tested in sea water. Internal water volume of the cell was 2.9 $cm.^3$, and flow rate through the cell during testing was 0.24 l/hr.

Sea water was obtained from the F.A.U. Marine Materials and Corrosion Laboratory and transported to the on-campus fatigue laboratory in plastic carboys approximately 24 hours before testing. This site of water collection is directly on the Atlantic Ocean at a location free of urban or industrial run-off, thus assuring that the test electrolyte was unpolluted. The water procurement operation involved filtering through sand to remove fouling organisms. Salinity of each collection was approximately 35.0 ppt.

For cathodic polarization tests a Pt-coated niobium counterelectrode strip was mounted to each side of the sea water bath and a port included for access to a saturated calomel electrode. Specimens were polarized to -0.78 v SCE (-0.85 volts, $Cu\text{-}CuSO_4$) by a potentiostat constructed from a circuit board obtained from Englehard Industries. Electrical contact to the specimen was provided by a solder connection external to the sea water bath.

Test Technique

Fatigue tests were performed on a MTS servohydraulic unit, series 812, operating in the load control mode on the 907 newton (2000 lb.) range.

Precracking was at 10 hz and $R = 0$ and proceeded until a crack extended to 2.54 mm. The technique involved sequencial load reduction in ten precent increments, according to the technique described by Nordmark and Fricke[1], such that a growth rate of 2.54×10^{-4} mm/cycle (10^{-6} inches/cycle) developed over the last 1.27 mm of precracking. This same load shedding increment was also employed subsequent to precracking.

Crack length was measured by one or both of two techniques. The first involved visual examination with a 30X, extended focal length microscope and calibrated eyepiece, while the second employed an extensiometer mounted upon the specimen and interfaced with the MTS unit. Resultant COD readings were translated to crack length from an experimentally determined compliance curve, which is presented in Figure 2. Also indicated for comparison purposes are curves projected by Hudak et al[2], based upon an analytical analysis.

Stress intensity was calculated as a function of crack length from the expression[3]

$$K = [P/(BW)^{1/2}][29.6(a/W)^{1/2} - 185.5(a/W)^{3/2} + 655.7(a/W)^{5/2} - 1017(a/W)^{7/2} + 638.9(a/W)^{9/2}], \quad (1)$$

where: P = applied load (newtons),

B = specimen thickness (mm),

W = specimen length (mm) and

a = crack length (mm).

Fatigue crack growth rates were determined at stress ratios (R) of 0.1 and 0.8 in air, freely corroding in sea water and cathodically protected in sea water. The stress function was a positive sinewave, and frequency was 60 Hz. The latter value was rounded from a calculation of guy wire strumming frequency from the relationship*

$$\text{Frequency (Hz)} = 0.313 \times \text{wind velocity (km/hr.)/cable diameter (cm.)}, \qquad (2)$$

assuming a 1.91 cm. (0.75 in.) diameter cable and 24.14 kilometer per hour wind.

* Equation provided by Mr. T. J. Dawson, NAVFAC.

EXPERIMENTAL RESULTS

Table III lists specimens which were tested as a part of this program and details test conditions and potential range for both freely corroding and cathodically polarized specimens.

Figures 3 through 5 present plots of fatigue crack growth rate versus stress intensity range for air, freely corroding and cathodically polarized tests at R = 0.1. Figures 6 through 8 detail the same data for R = 0.8. Limited data at 10 Hz under freely corroding conditions is also included in Figure 4. While this indicates a slight increase in fatigue crack growth rate with reduced frequency, it is not clear that the difference between the two curves exceeds expected specimen-to-specimen scatter.

Best fit curves from the above figures are superimposed in Figure 9, thus facilitating a relative comparison for the different environments and stress ratios. Apparent from Figure 9 is a generalized shift in crack growth rate to higher values (constant ΔK) as R was increased from 0.1 to 0.8. Such a change is consistent with data from previous low stress intensity range investigations. Figure 9 indicates further that da/dN in air exceeded that in sea water, either freely corroding or cathodically protected. Relative slopes of the three curves suggests, however, that da/dN for air and freely corroding tests in sea water approach one another at high stress intensity ranges (~ 22 $MPa \cdot m^{\frac{1}{2}}$). Similarly, above approximately 10 $MPa \cdot m^{\frac{1}{2}}$ crack growth rate under freely corroding conditions exceeded that where the specimen was cathodically polarized. Below this stress intensity range the trend reversed. If the -0.78 v, SCE, curve is extrapolated to lower stress intensities, merger with the air data near 10 $MPa \cdot m^{\frac{1}{2}}$ is indicated. This lower limit of sea water crack growth rate data reflects difficulty in crack length determinations in this region. However, the lowest stress intensity range data in Figure 5 suggests a threshold is being approached; and if this is the case, then merger of air and cathodically polarized crack growth rate curves, as projected above, may nor occur.

For R = 0.8 the freely corroding and cathodically polarized da/dN data exceed the air values at stress intensity ranges of 7.5 and 9.0 $MPa \cdot m^{\frac{1}{2}}$, respectively. Below these crack growth rates in air are the greatest. Interestingly, for da/dN values below 4×10^{-6} mm/cycle crack growth rate for cathodically protected specimens at R = 0.1 was greater than for freely corroding ones, but for R = 0.8 the freely corroding fatigue crack extended more rapidly.

That fatigue crack growth rate in air can, under certain conditions, exceed that in sea water has also been observed by previous investigators[4-6]. Vosikovsky[5] and Tu and Seth[6] have attributed this finding to crack branching, as induced by some form of hydrogen embrittlement. Such multiple cracking should result in reduced effective stress intensity in the vicinity of the crack tip.

To determine if crack branching might have contributed to low fatigue crack growth rates in the present sea water tests several specimens were sectioned, polished and examined metallographically at magnifications up to 400X; however no multiple crack paths were disclosed. Supplementary fractographic observations employing scanning electron microscopy also did not reveal secondary cracks.

Figures 10 through 12 reproduce $R = 0.1$ data for the present study (Figures 3 through 5) in perspective to results of earlier studies[7,8] upon HY-80 steel under similar test conditions but at higher stress intensity range. In all three instances the agreement of data from the different investigators is good.

Comparison of present threshold data with that of other steels is important in rationalizing suitability of HY-80 as an alternative eyebolt material. In this regard Table III lists ΔK_{th} values, as reported in the literature[2,5,6,9-11], for a variety of steels fatigued in air. Comparison for the air environment is appropriate since threshold values for this test situation were less than for either freely corroding or cathodically polarized conditions (Figures 4 and 5). Also included are data from the present investigation.

Rolfe and Barsom[12] have analyzed ΔK_{th} data as a function of stress ratio for various steels and have determined the lower bound to conform to the equation

$$\Delta K_{th}(ksi \cdot in^{\frac{1}{2}}) = 6.4(1 - 0.85R). \qquad (3)$$

A similar correlation has been projected by O. Vosikovsky et al[5]. Figure 13 presents a ΔK_{th}-R plot illustrating the scatter band of data considered by Rolfe and Barson in addition to the data in Table III. Considerable departure from the Rolfe-Barson trend is apparent, particularly at low stress ratio values.

Of interest to the present analysis is the fact that the ΔK_{th} value for HY-80 steel at R = 0.8, as determined in the present investigation, is greater than for the other steels which have been previously studied. This suggests that realizable benefits should result from selection of HY-80 steel in high static stress, low stress range applications, such as the guy wire anchor bolt one discussed earlier.

BIBLIOGRAPHY

1. G. E. Nordmark and W. G. Fricke, "Fatigue Crack Arrest at Low Stress Intensity Range in Corrosive Environment", Report No. 57-78-02, Alcoa Laboratories (1978).

2. S. J. Hudak, A. Saxema, R. J. Bucci and R. C. Malcolm, "Development of Standard Methods of Testing and Analyzing Fatigue Crack Growth Rate Data", Research Report 77-903-AFCGR-R1, Westinghouse Research and Development Center (1978), pp. 12 - 15.

3. E. T. Wessel, Engr. Fract. Mechanics, vol. 1 (1968), p. 77.

4. P. M. Scott and D. R. V. Silvester, "The Influence of Seawater on Fatigue Crack Propagation Rates in Structural Steel", Department of Energy, UK Offshore Steels Research Project. Technical Interim Report UKOSRP 3/03, December, 1975.

5. O. Vosikovsky, "Fatigue Crack Growth in X-65 Line-Pipe Steel at Low Frequencies in Aqueous Environments", Closed Loop, vol. 6 (1976), pp. 3 - 12.

6. L. K. L. Tu and B. B. Seth, Journal of Testing and Evaluation, vol. 6 (1978), pp. 66 - 74.

7. J. M. Barsom, E. J. Imholf and S. T. Rolfe, Engr. Fracture Mechanics, vol. 2 (1971), pp. 301 - 317.

8. J. P. Gallagher, "Corrosion Fatigue Crack Growth Behavior Above and Below K_{ISCC}", NRL Report 7064, May, 1970.

9. R. J. Bucci, W. G. Clark, Jr. and P. C. Paris, Stress Analysis and Growth of Cracks, ASTM STP 513, ASTM, Philadelphia (1972), pp. 177 - 195.

10. R. J. Cooke and C. J. Beevers, Materials Science and Engineering, vol. 13 (1974), pp. 201 - 210.

11. P. C. Paris, R. J. Bucci, E. T. Wessel, W. G. Clark and T. R. Mager, Stress Analysis and Growth of Cracks, ASTM STP 513, ASTM, Philadelphia (1972) pp. 141 - 176.

BIBLIOGRAPHY (Cont'd. . .)

12. S. T. Rolfe and J. M. Barsom, Fracture and Fatigue Control in Structures - Applications of Fracture Mechanics, Prentice-Hall, Inc. Englewood Cliffs, New Jersey (1977) pp. 223 - 226.

TABLE I

CHEMICAL COMPOSITION OF HY-80 STEEL STOCK

C	Mn	Si	P	S	Cr	Ni	Mo	Cu	T	V
0.14	0.34	0.27	0.10	0.003	1.27	2.23	0.32	0.06	<0.02	<0.01

TABLE II

MECHANICAL PROPERTIES OF HY-80 STEEL STOCK

LOT NUMBER	SPECIMEN NUMBER	YIELD STRENGTH* MPa (ksi)	ULTIMATE STRENGTH MPa (ksi)	ELONGATION IN 5.08 CM (2 INCH) %	REDUCTION OF AREA %	CHARPY V-NOTCH IMPACT STRENGTH AT -46°C (-50°F**) nt-m (ft-lb)
K	2,6,7,8	550 (79.75) 550 (79.75)	672 (97.50) 672 (97.50)	29.0 (29.0) 27.0 (27.0)	77.0 77.0 74.9 74.9	248 (183) 248 (183)
L	1,3,4,5	563 (81.70) 563 (81.70)	686 (99.50) 694 (100.70)	28.0 (28.0) 28.0 (28.0)	78.3 78.3 78.3 78.3	243 (179.5) 243 (179.5)

* 0.2% Offset

** Average of 4 Tests

TABLE III

LISTING OF TEST VARIABLES FOR FATIGUE SPECIMENS

SPECIMEN NUMBER	ENVIRONMENTAL CONDITIONS	LOWEST READING ϕ sce (volts)	MEAN READING ϕ sce (volts)	HIGHEST READING ϕ sce (volts)
1,2	Air			
3	Freely Corroding	-.556	-.611	-.681
4	Freely Corroding	-.502	-.631	-.726
5	Cathodically Protected	-.776	-.776	-.778
6	Cathodically Protected	-.776	-.779	-.800*
7	Cathodically Protected	-.777	-.781	-.784
8	Cathodically Protected	-.776	-.779	-.802*
8	Freely Corroding**	-.568	-.647	-.683

* Minimum value before test was discontinued due to potential fluctuations.

** Loading frequency of 10 Hz; all other tests conducted at 60 Hz.

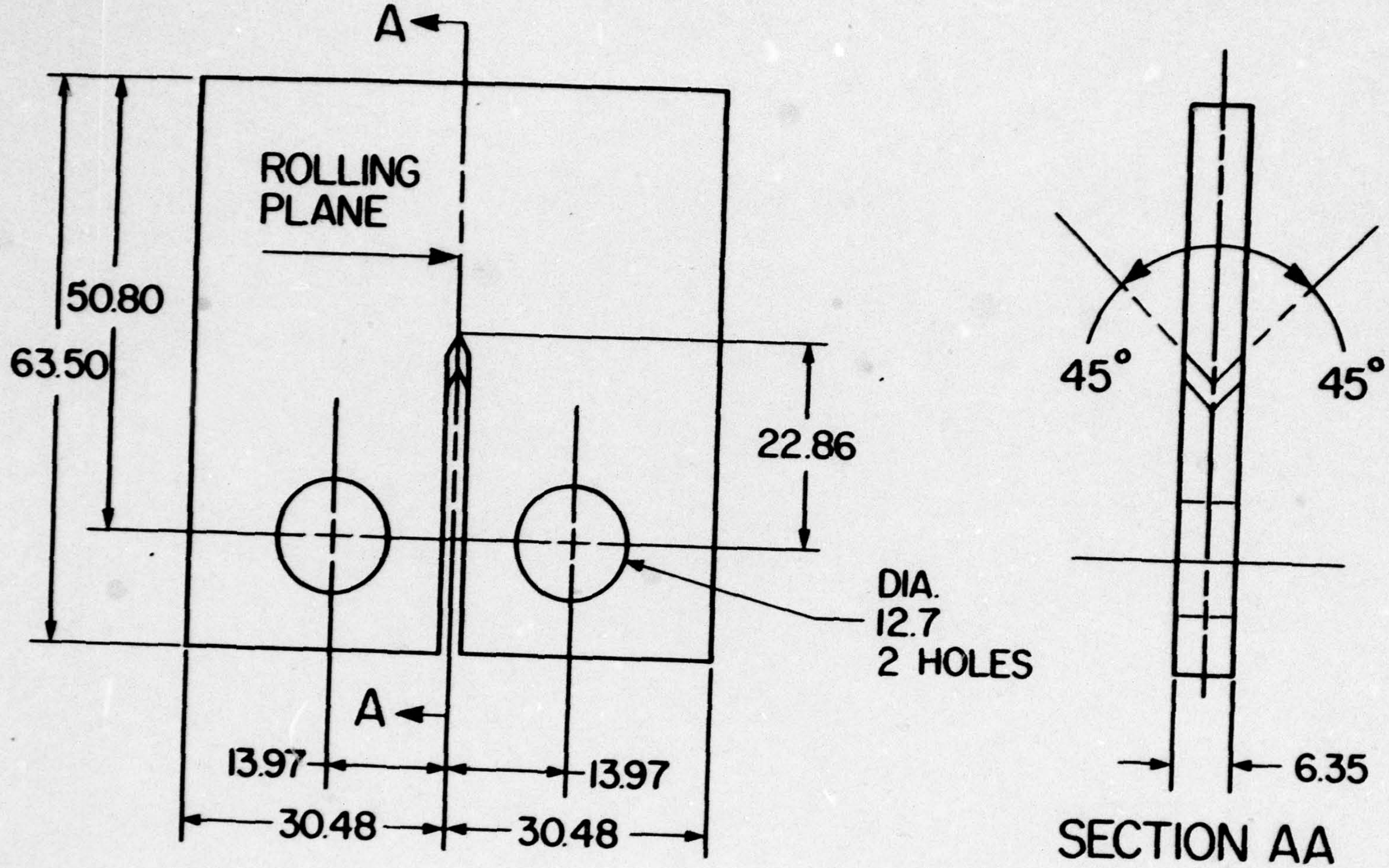

NOTE 1: Notch width is 2.38mm.
NOTE 2: All dimensions are in millimeters

FIGURE 1: GEOMETRY OF COMPACT TENSION SPECIMENS EMPLOYED IN FATIGUE TESTS.

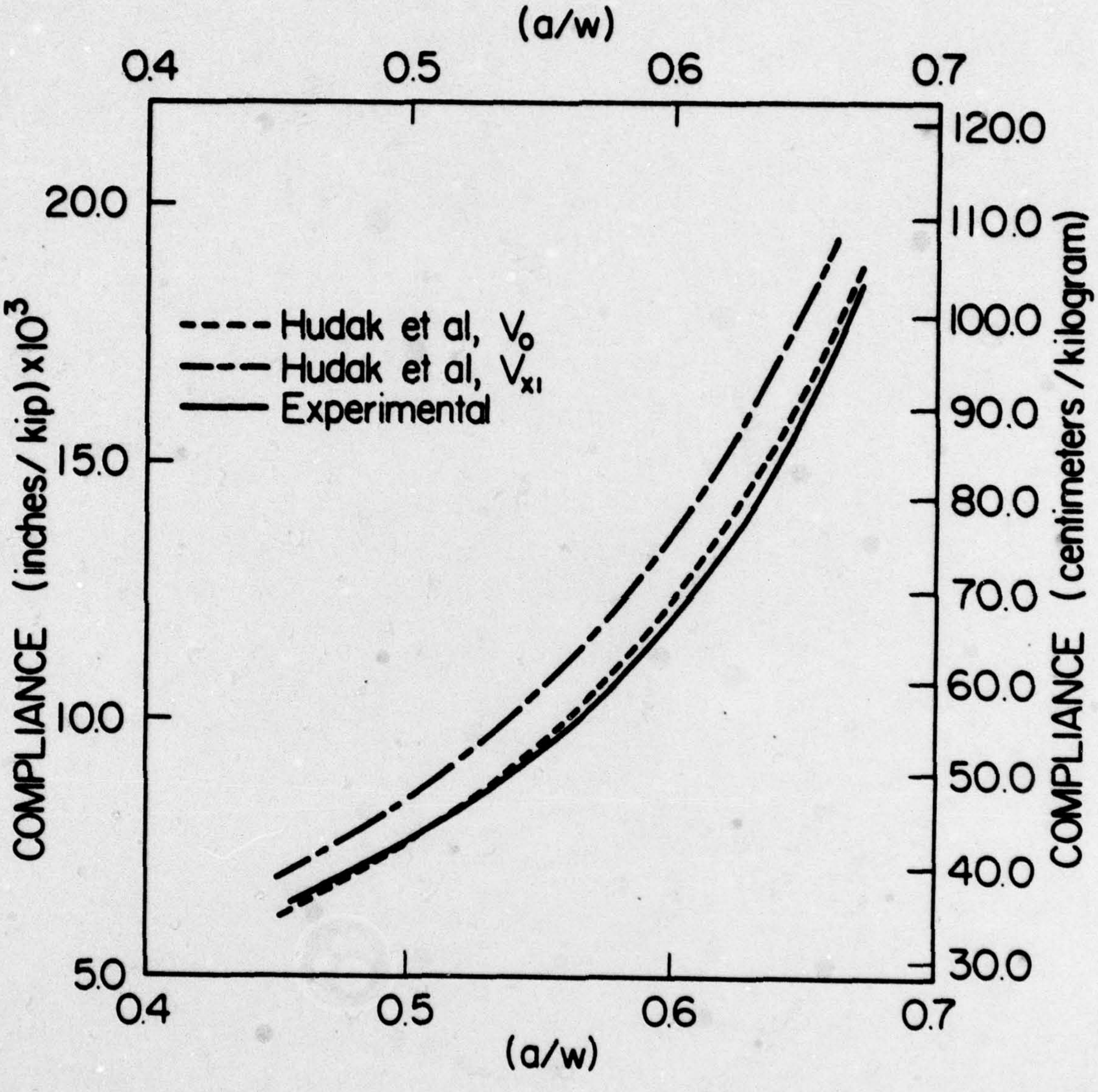

FIGURE 2: COMPLIANCE VERSUS CRACK LENGTH RELATIONSHIP FOR THE PRESENT SPECIMEN.

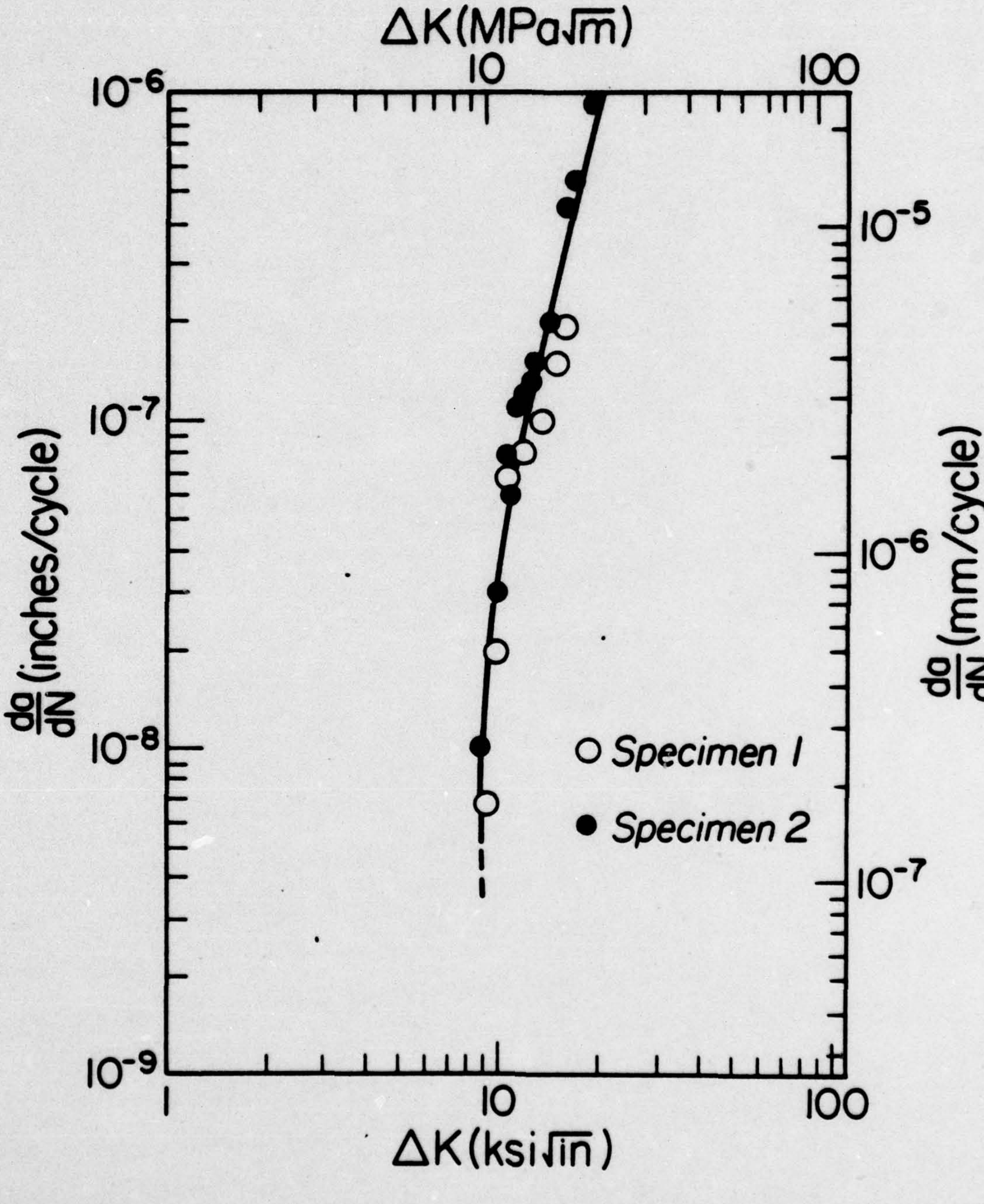

FIGURE 3: FATIGUE CRACK GROWTH RATE VERSUS STRESS INTENSITY RANGE FOR HY-80 STEEL IN AIR WITH R = 0.1.

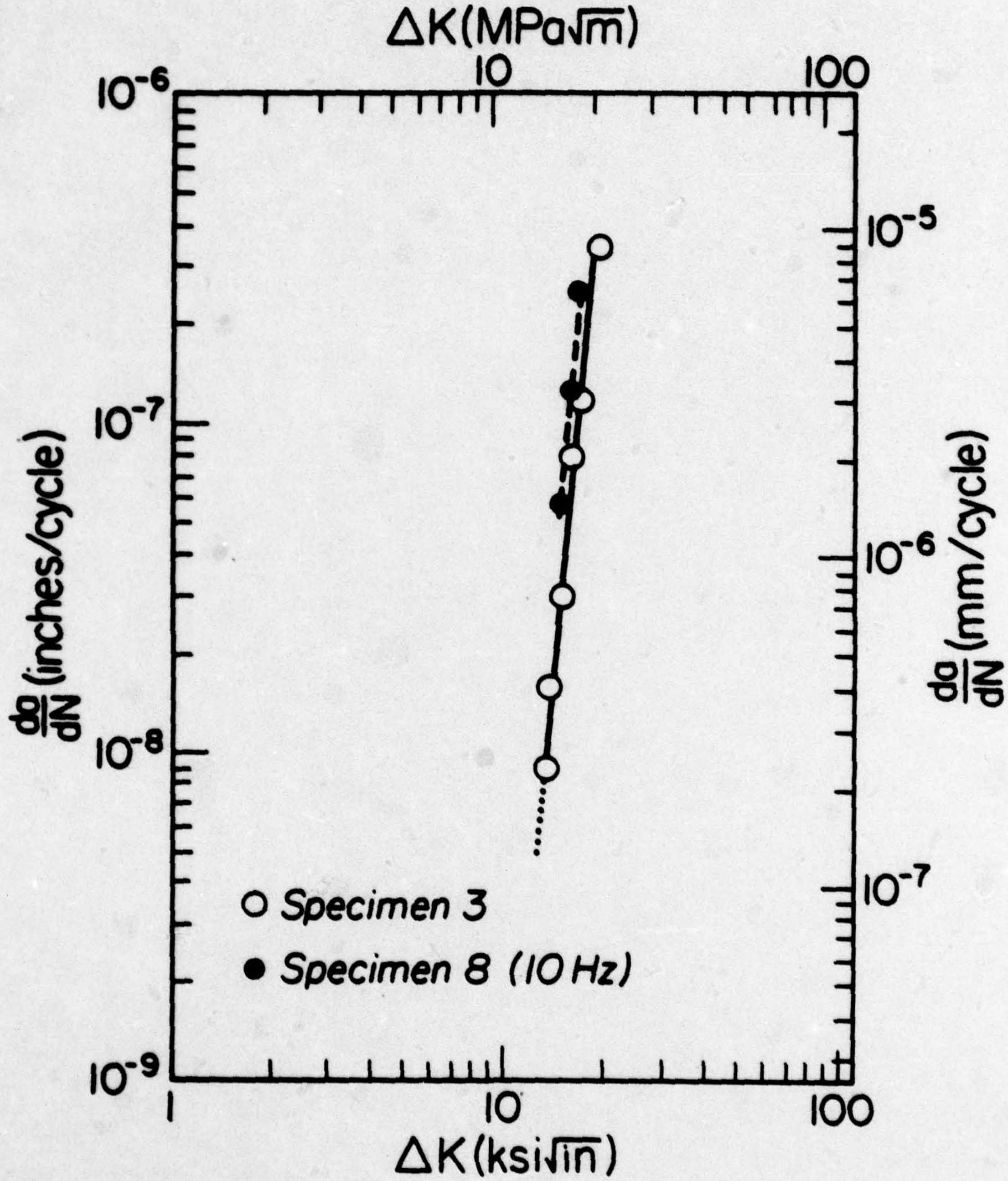

FIGURE 4: FATIGUE CRACK GROWTH RATE VERSUS STRESS INTENSITY RANGE FOR HY-80 STEEL FREELY CORRODING IN SEA WATER WITH R = 0.1.

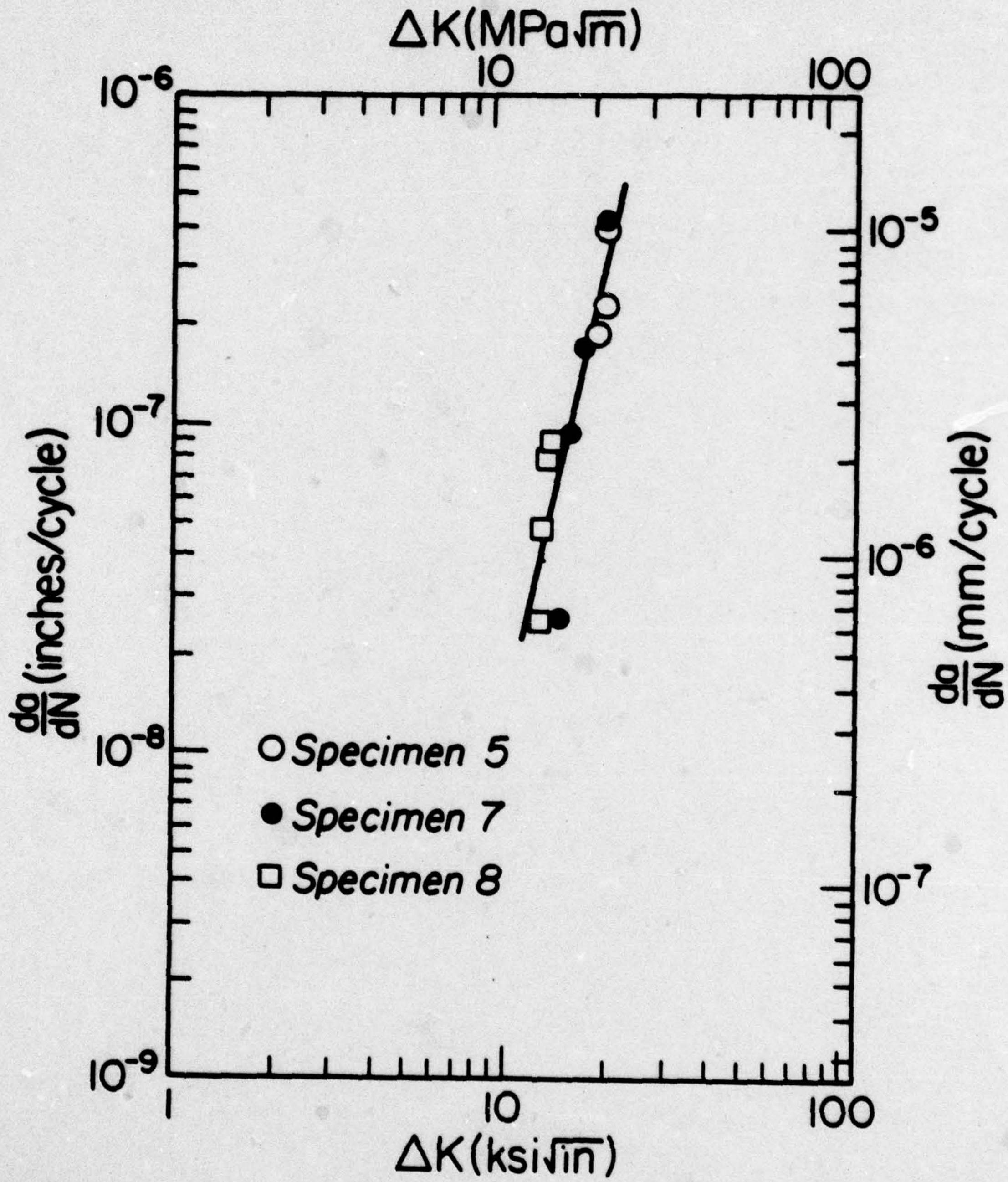

FIGURE 5: FATIGUE CRACK GROWTH RATE VERSUS STRESS INTENSITY RANGE FOR HY-80 STEEL CATHODICALLY POLARIZED IN SEA WATER TO -0.85 VOLTS, Cu-$CuSO_4$, WITH R = 0.1.

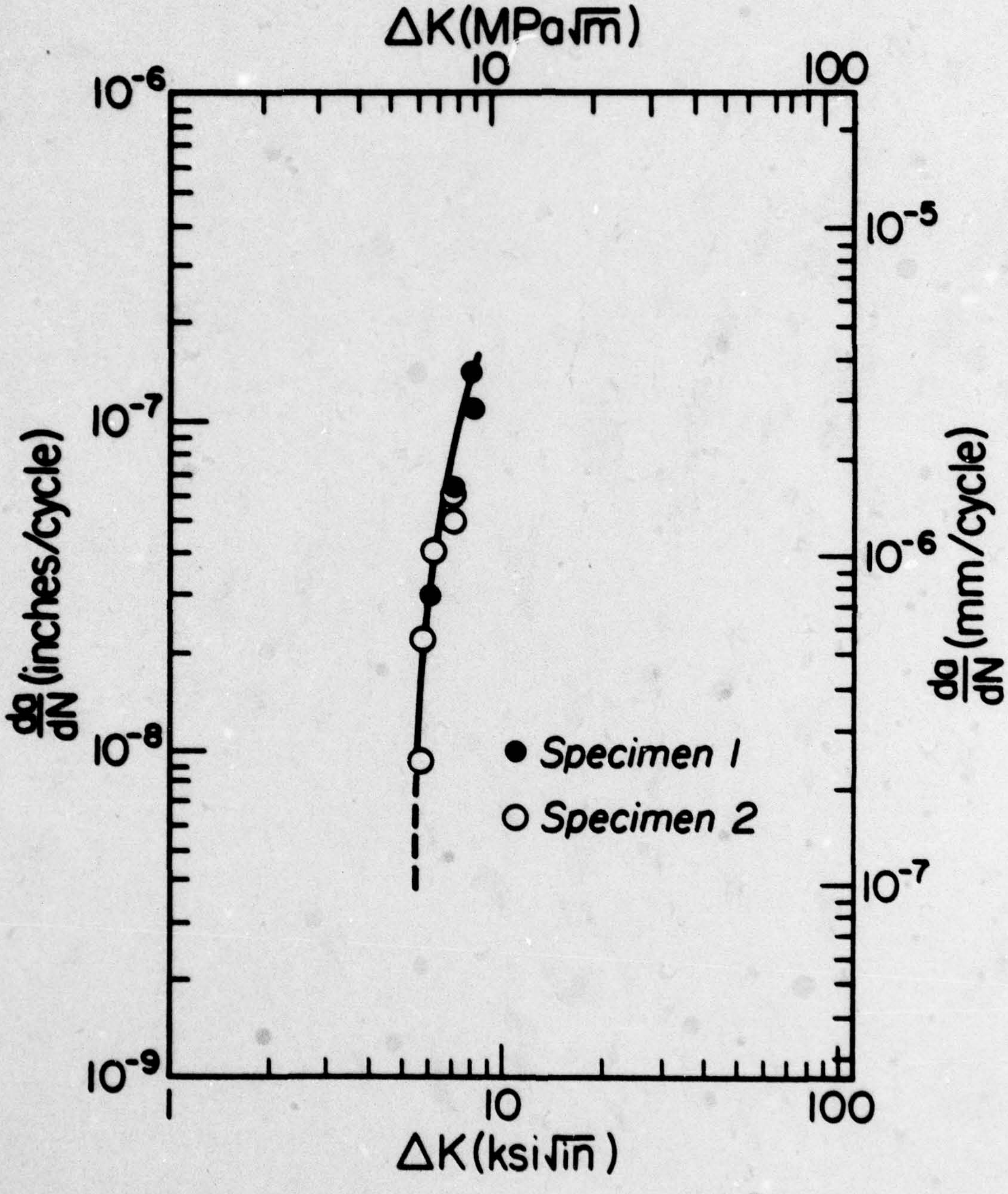

FIGURE 6: FATIGUE CRACK GROWTH RATE VERSUS STRESS INTENSITY RANGE FOR HY-80 STEEL IN AIR WITH R = 0.8.

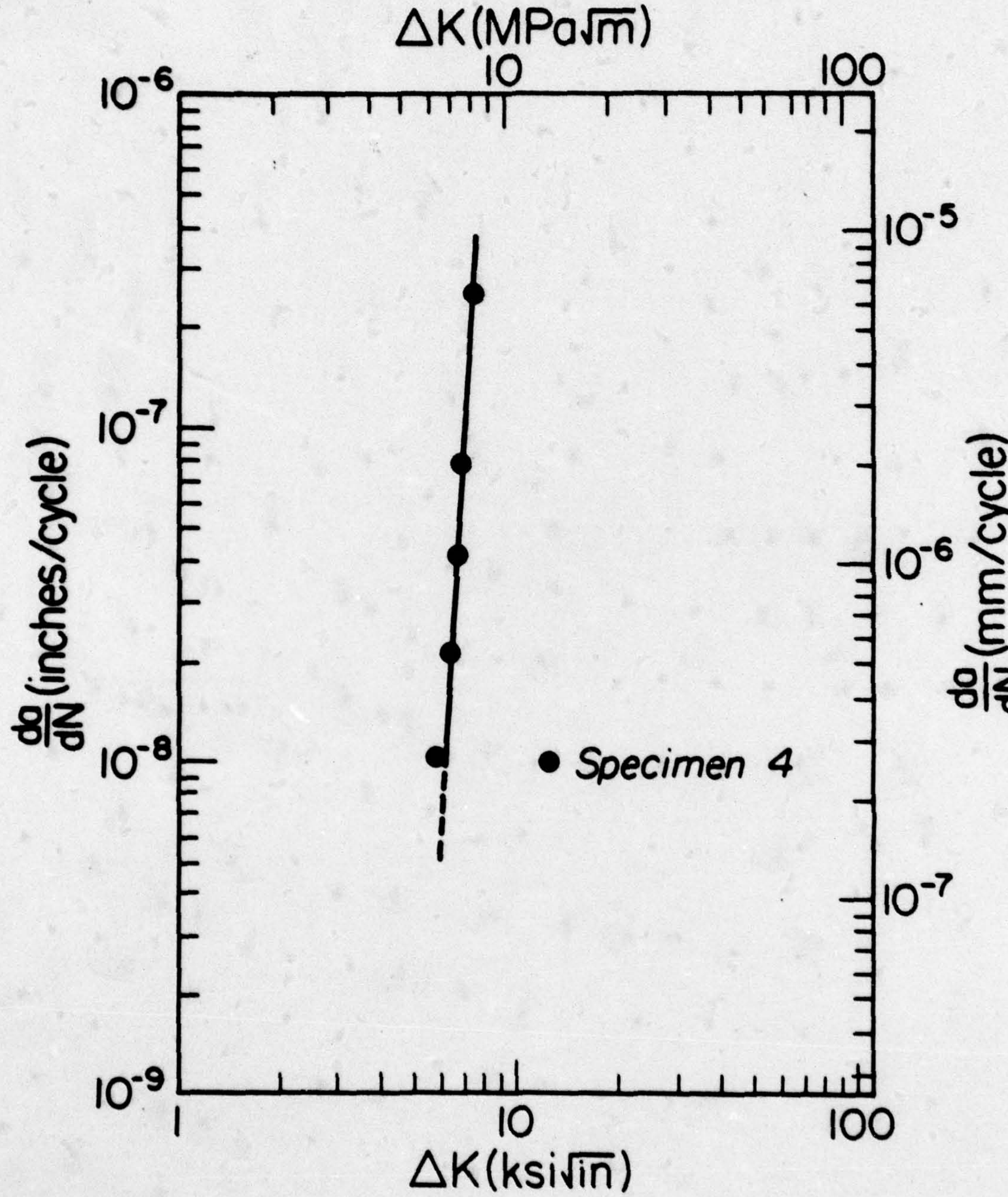

FIGURE 7: FATIGUE CRACK GROWTH RATE VERSUS STRESS INTENSITY RANGE FOR HY-80 STEEL FREELY CORRODING IN SEA WATER WITH R = 0.8.

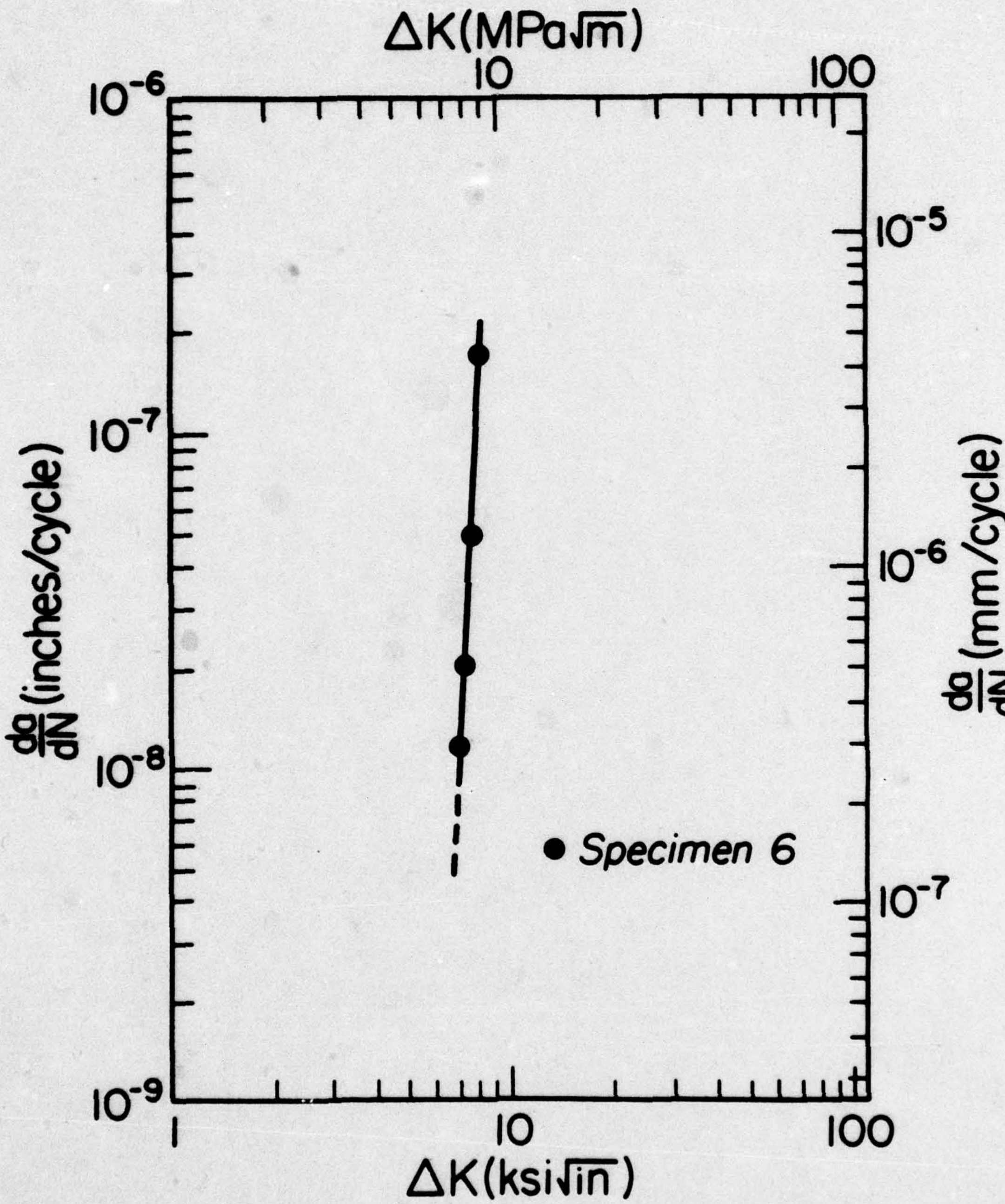

FIGURE 8: FATIGUE CRACK GROWTH RATE VERSUS STRESS INTENSITY RANGE FOR HY-80 STEEL CATHODICALLY POLARIZED IN SEA WATER TO -0.85 VOLTS, $Cu\text{-}CuSO_4$, WITH R = 0.8.

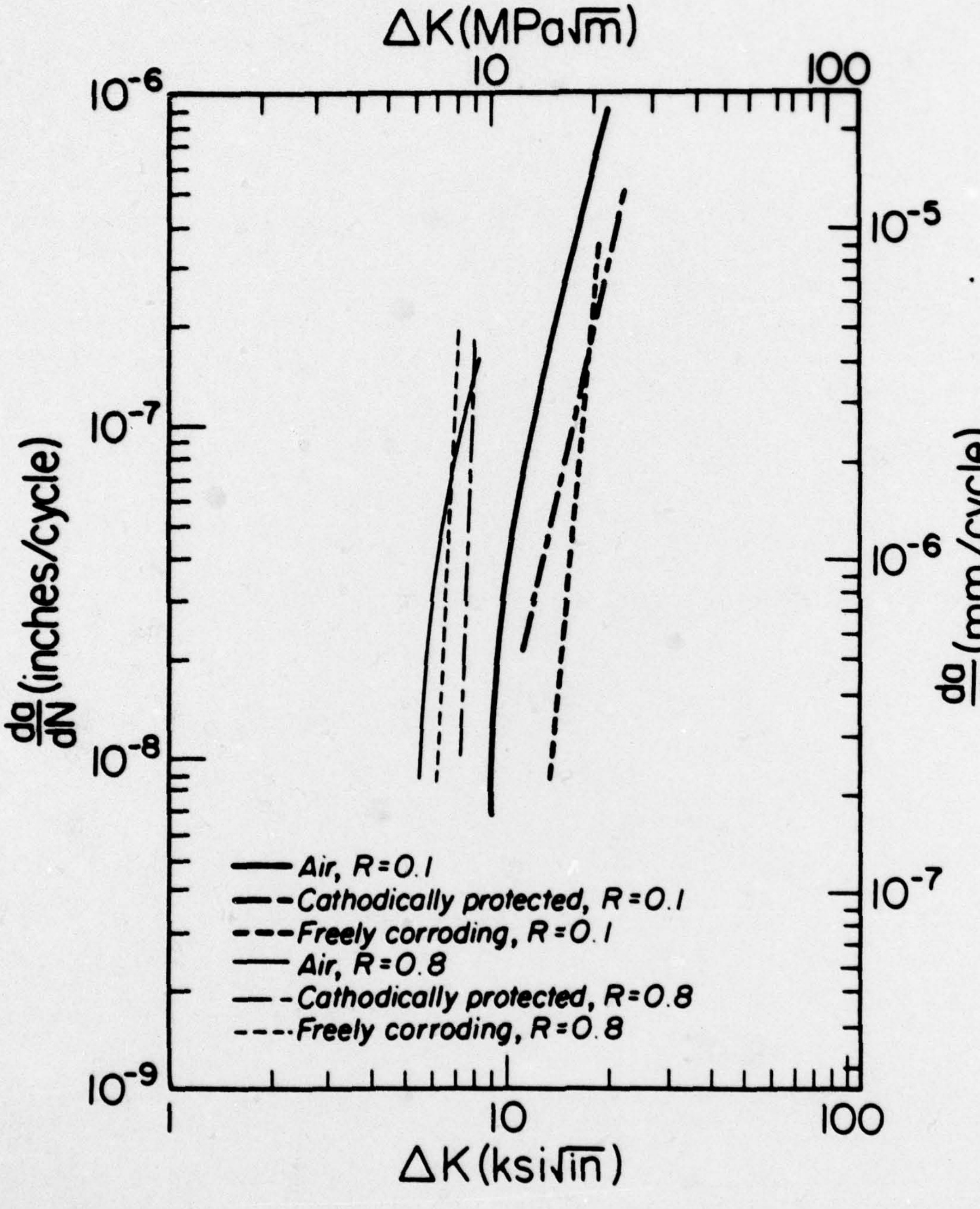

FIGURE 9: COMPARISON OF FATIGUE CRACK GROWTH RATE PROPERTIES FOR HY-80 STEEL IN AIR AND SEA WATER WITH R = 0.1 AND 0.8.

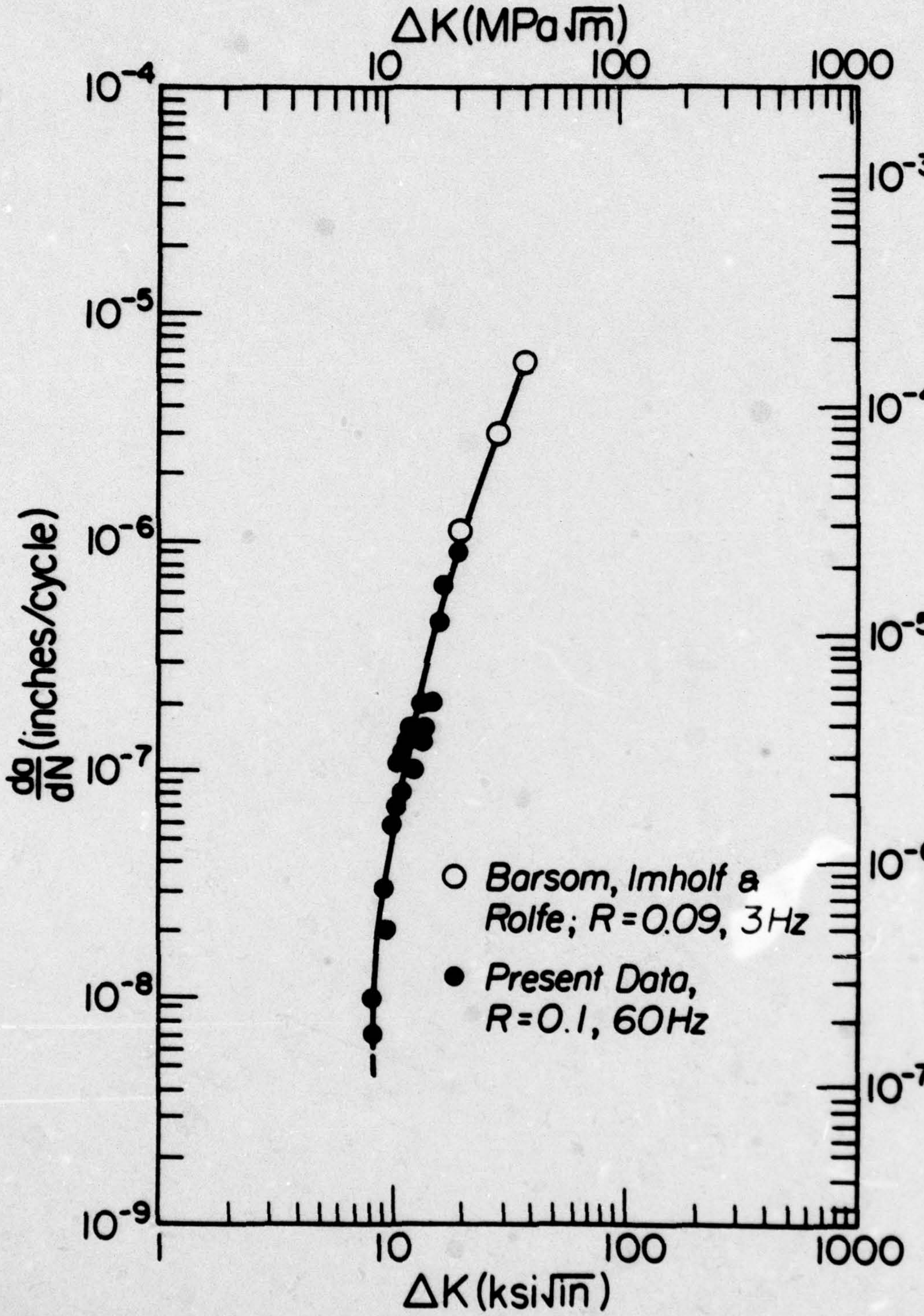

FIGURE 10: COMPARISON OF FATIGUE CRACK GROWTH RATES FROM DIFFERENT INVESTIGATIONS FOR HY-80 STEEL TESTED IN AIR.

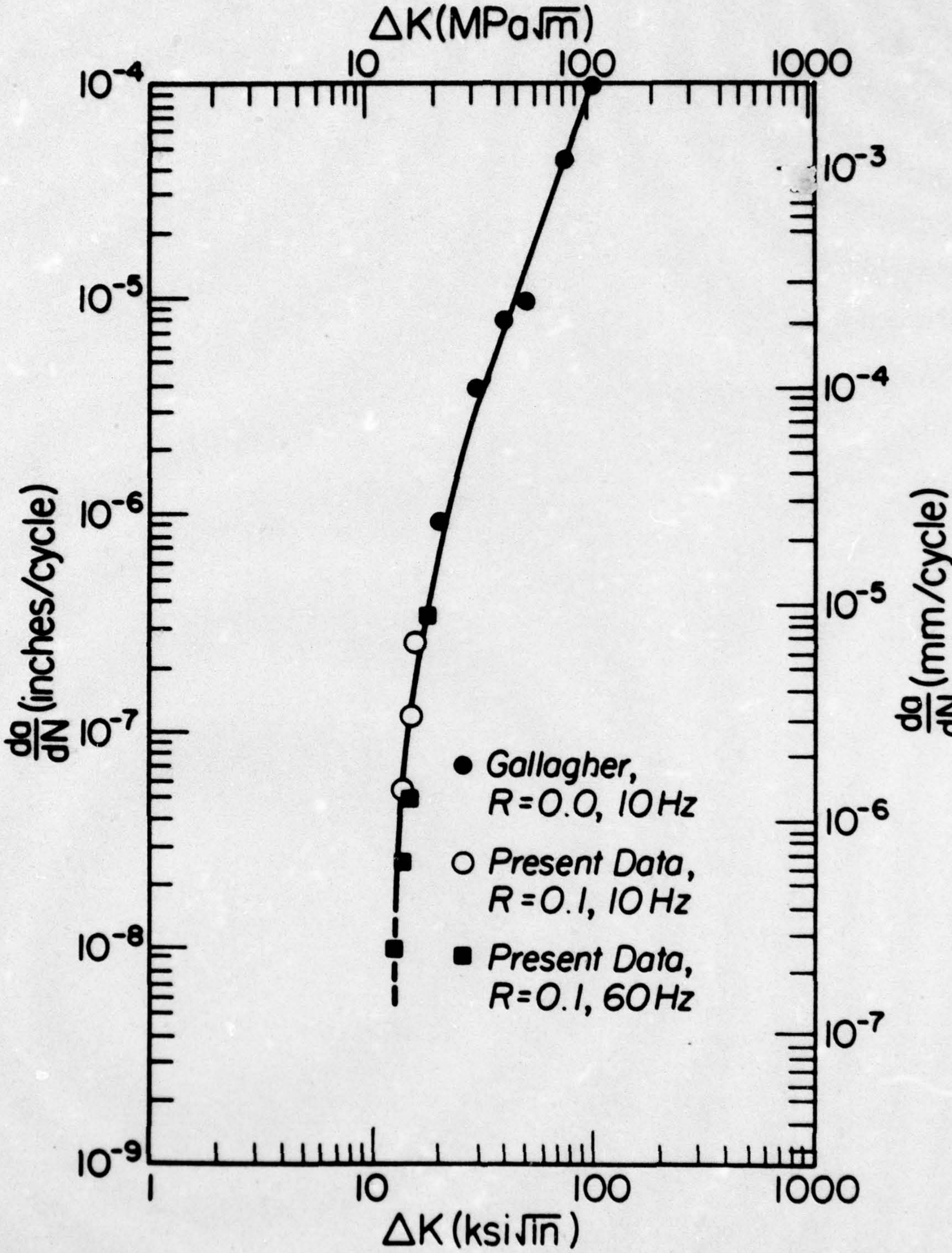

FIGURE 11: COMPARISON OF FATIGUE CRACK GROWTH RATES FROM DIFFERENT INVESTIGATIONS FOR HY-80 STEEL TESTED IN SEA WATER OR SALT WATER.

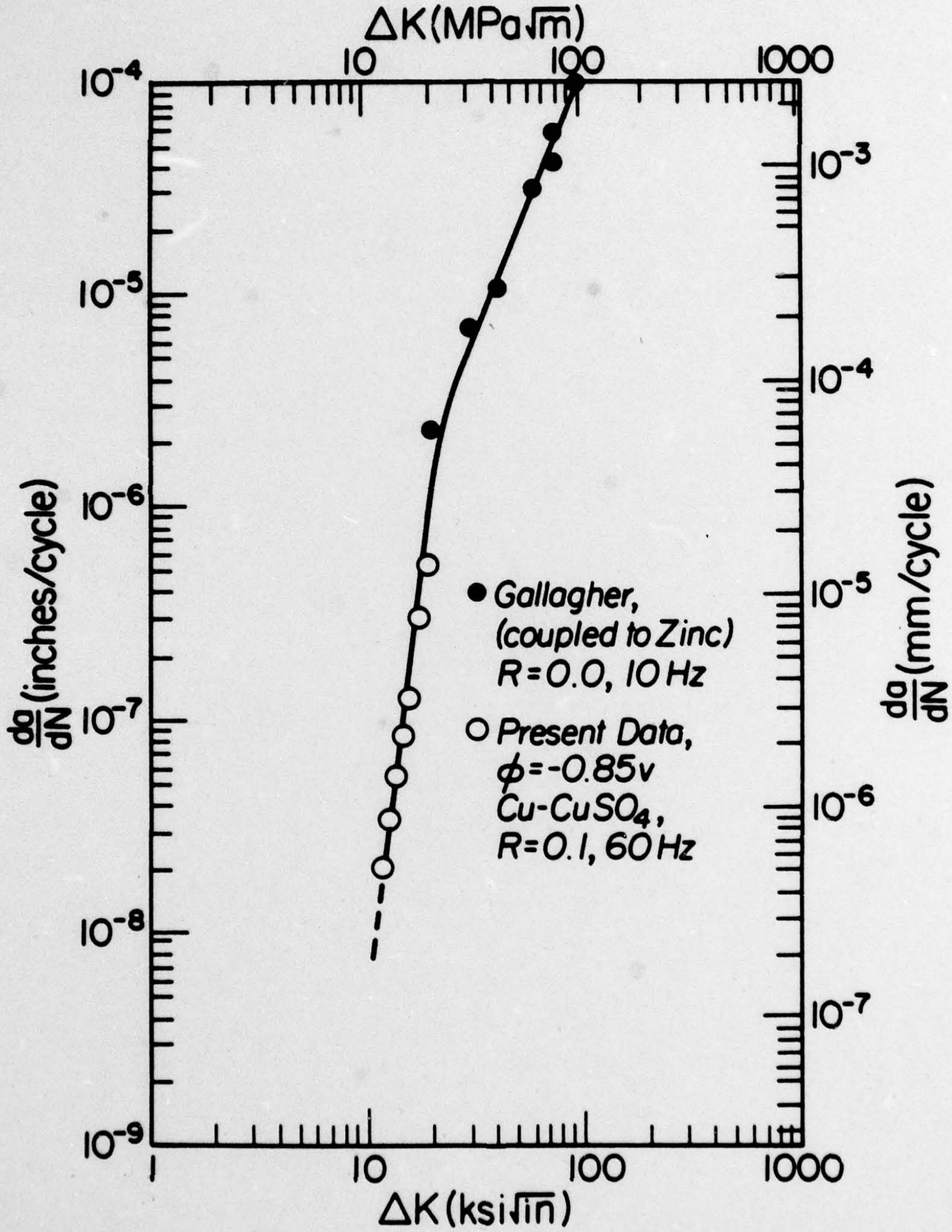

FIGURE 12: COMPARISON OF FATIGUE CRACK GROWTH RATES FROM DIFFERENT INVESTIGATIONS FOR HY-80 STEEL CATHODICALLY POLARIZED IN SEA WATER OR SALT WATER.

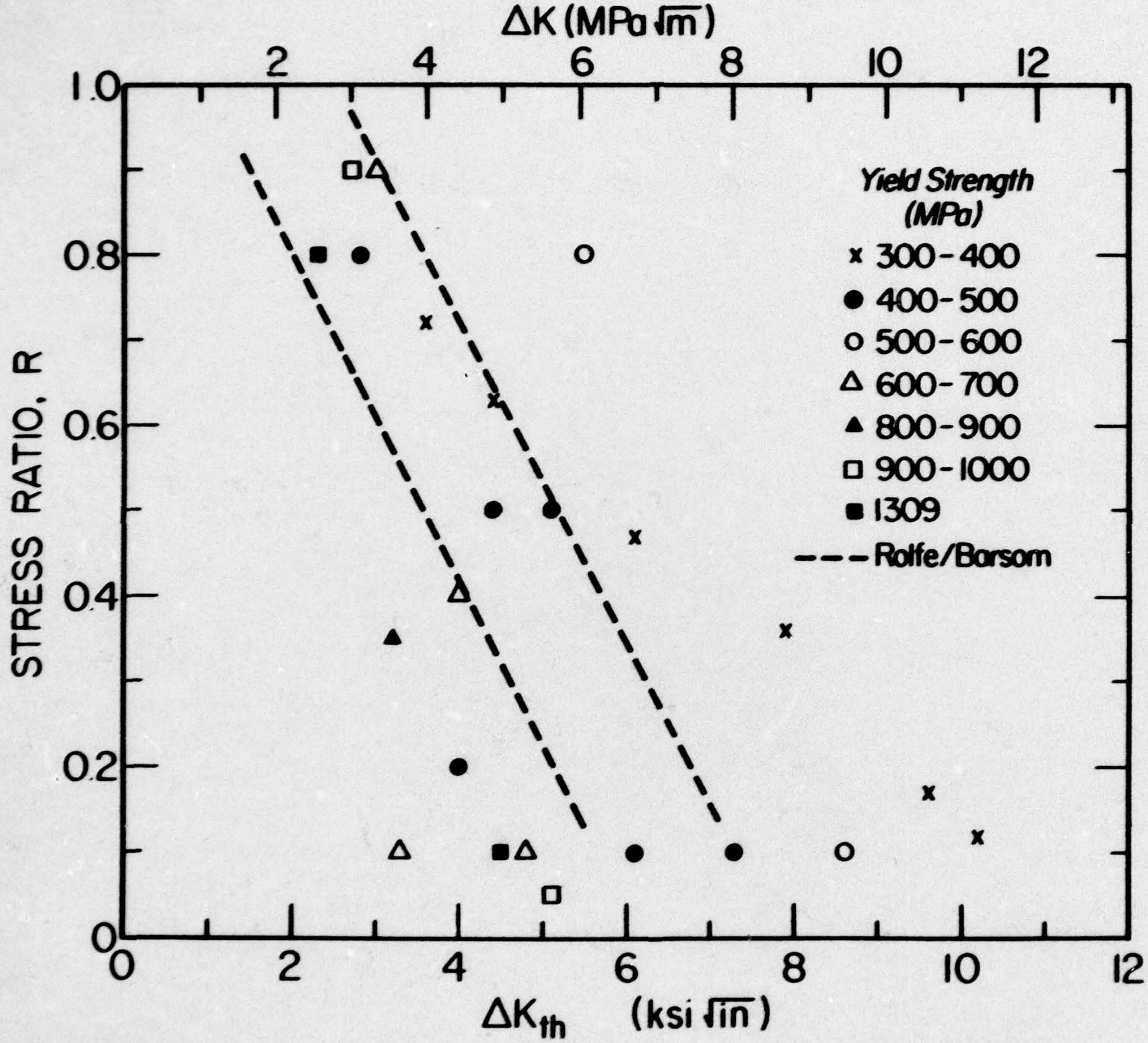

FIGURE 13: PLOT OF THRESHOLD STRESS INTENSITY RANGE VERSUS STRESS INTENSITY RATIO FOR VARIOUS STEELS IN AIR.